Acta Crystallographica Section C
Crystal Structure Communications
ISSN 0108-2701

5,5′-Di-*tert*-butyl-2,2′-dihydroxy-3,3′-methanediyldibenzaldehyde and its allyl-protected dialcohol and dialdehyde precursors

Sandrine Goetz, Julia Barreira Fontecha and Vickie McKee*

Chemistry Department, Loughborough University, Leicestershire LE11 3TU, England
Correspondence e-mail: v.mckee@lboro.ac.uk

Received 9 August 2004
Accepted 24 August 2004
Online 9 October 2004

5,5′-Di-*tert*-butyl-2,2′-dihydroxy-3,3′-methanediyldibenzaldehyde, $C_{23}H_{28}O_4$, (IV), has been structurally characterized in two polymorphic forms. The tetragonal form, (in $I4_1/a$) has been reported previously but is redetermined and reinterpreted here, while the monoclinic form, (in $C2/c$) is reported for the first time. In both polymorphs, the molecule lies on a crystallographic twofold axis. Two precursors in the synthesis of (IV), namely 2,2′-bis(allyloxy)-5,5′-di-*tert*-butyl-3,3′-methanediyldibenzenemethanol ($C_{29}H_{40}O_4$) and 2,2′-bis(allyloxy)-5,5′-di-*tert*-butyl-3,3′-methanediyldibenzaldehyde ($C_{29}H_{36}O_4$) have also been characterized.

Comment

The diphenolic dialdehyde 5,5′-di-*tert*-butyl-2,2′-dihydroxy-3,3′-methanediyldibenzaldehyde, (IV), has been used to synthesize new polynucleating macrocycles by Schiff base condensation with diamines (Barreira Fontecha *et al.*, 2002). Compound (IV) was prepared in three steps from the known dialcohol analogue 5,5′-di-*tert*-butyl-2,2′-dihydroxy-3,3′-methanediyldibenzenemethanol, (I) (Dhawan & Gutsche, 1983).

The structure of 2,2′-bis(allyloxy)-5,5′-di-*tert*-butyl-3,3′-methanediyldibenzenemethanol, (II), is shown in Fig. 1. The molecule is non-planar, with the two aryl rings inclined at 78.84 (9)° with respect to one another and the *tert*-butyl groups lying on opposite sides of the molecule. The apparent folding of the molecule is actually due to rotation about the C12—C4 and C12—C13 bonds, and the conformation adopted is probably a consequence of the hydrogen-bonding network throughout the lattice. Hydrogen bonding between alcohol groups generates eight-membered rings [graph-set notation $R_4^4(8)$] and links the molecules into a double chain running parallel to the *a* axis (Fig. 2 and Table 1). The H atoms on the hydroxy groups are disordered, and these atoms were modelled with 50% occupancy of two equivalent positions. As a result there are two self-consistent hydrogen-bonding patterns, which have O—H⋯O directions running either anticlockwise (as in Fig. 2) or clockwise around the same ring. The highest residual electron-density peak is 1.26 Å from atom C28 and 1.39 Å from atom C27, and may indicate a minor disorder of that allyl group.

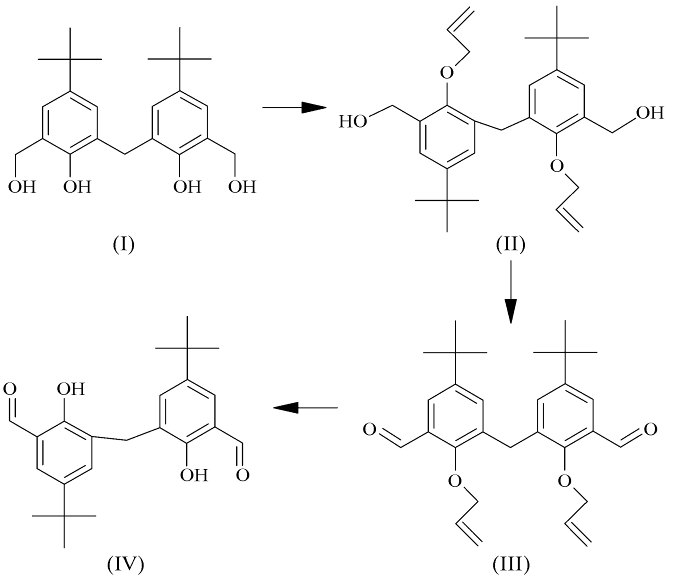

The dialcohol was oxidized using MnO_2 to form the analogous dialdehyde, 2,2′-bis(allyloxy)-5,5′-di-*tert*-butyl-3,3′-methanediyldibenzaldehyde, (III). As Fig. 3 shows, the phenyl planes are inclined at 74.17 (5)° and the *tert*-butyl groups are on the same side of the molecule. One of the allyl groups is disordered, and this disorder was modelled as a 70:30 occupancy of two conformations. Again, the molecules are linked by hydrogen bonding into a double chain, in this case running

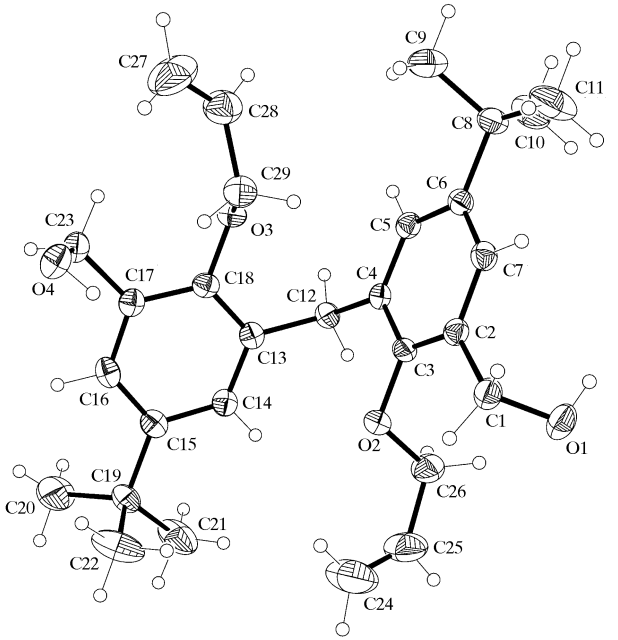

Figure 1
A view of the structure of (II). The H atoms on the two alcohol functions are disordered and only one position is shown for each. Displacement ellipsoids are drawn at the 50% probability level.

DOI: 10.1107/S010827010402089X

parallel to *c* (Fig. 4); however, the interactions are all of the type C—H···O═C (Table 2). There is also some π–π stacking across the hydrogen-bonded chain involving the benzaldehyde groups. The section incorporating atoms O1/C1/C2/C3/C7 overlaps the O4/C23/C16–C18 section of a neighbouring molecule at (x, $\frac{1}{2} - y$, $\frac{1}{2} + z$). The planes of the interacting benzaldehyde rings are inclined at 12.33 (7)°, while atoms O1 and C1 are 3.274 (2) and 3.357 (2) Å, respectively, from the mean plane of the interacting phenyl ring (Fig. 4).

Compound (IV) has been characterized in two polymorphic forms. We obtained the tetragonal form, (IV*a*) (space group $I4_1/a$), by recrystallization of the crude material from diethyl ether, while Masci *et al.* (2004) obtained the same polymorph by recrystallization from methanol. A second polymorph was formed as a side product in the synthesis of a macrocyclic complex; crystals of (IV*b*) in the monoclinic space group *C*2/*c* were obtained from a methanol solution containing 1,5-diaminopentan-3-ol and nickel(II) nitrate.

In the tetragonal form, (IV*a*), the asymmetric unit contains half of the molecule, with a twofold axis passing through atom C12 (Fig. 5), while in the monoclinic form, (IV*b*), the asymmetric unit contains two independent half molecules, each having twofold symmetry (Fig. 6). The molecular conformation and bond lengths are similar in the two polymorphs; the *tert*-butyl groups are on opposite sides of the linked aryl rings and the phenol H atoms are involved in intramolecular hydrogen bonds with the adjacent carbonyl groups (Tables 3 and 4). In (IV*b*), there is additional intermolecular hydrogen bonding involving one of the carbonyl groups (C13═O3). Atom C13 forms a C—H···O═C hydrogen bond to atom O3 of a neighbouring molecule at ($-x$, $2 - y$, $1 - z$), resulting in zigzag chains parallel to *c*. The second molecule does not show a corresponding interaction. As in the precursors, the phenyl rings are inclined with respect to one another: in the tetragonal form, the phenyl rings are inclined at 61.48 (5)°, whereas in the monoclinic polymorph, the values are 73.58 (5) and 75.04 (5)°.

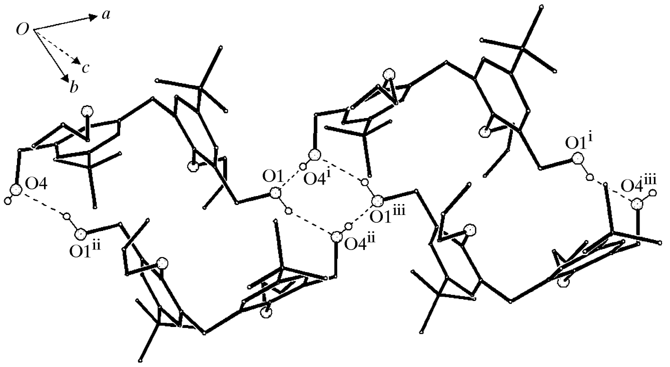

Figure 2
The hydrogen bonding in (II), producing a double chain parallel to *a*. Only one of the two orientations of the hydrogen bonding within the $R_4^4(8)$ ring is shown. [Symmetry codes: (i) $1 + x$, y, z; (ii) $-x$, $2 - y$, $-z$; (iii) $1 - x$, $2 - y$, $-z$.]

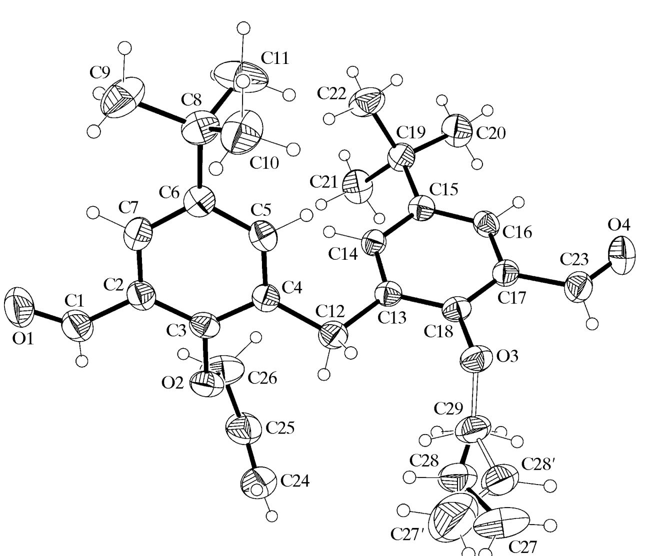

Figure 3
A view of the structure of (III), showing the disorder in one allyl group. Displacement ellipsoids are drawn at the 50% probability level.

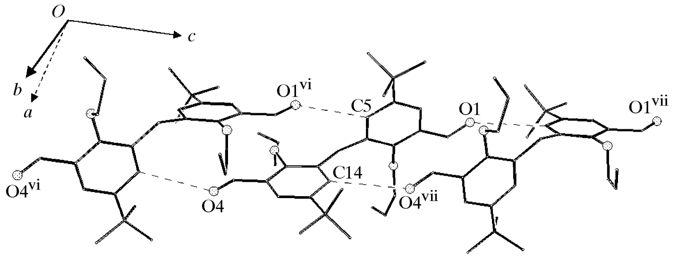

Figure 4
The C—H···O═C hydrogen-bonded chain parallel to *b* in (III). [Symmetry codes: (vi) x, $\frac{1}{2} - y$, $\frac{1}{2} + z$; (vii) x, $\frac{1}{2} - y$, $-\frac{1}{2} + z$.]

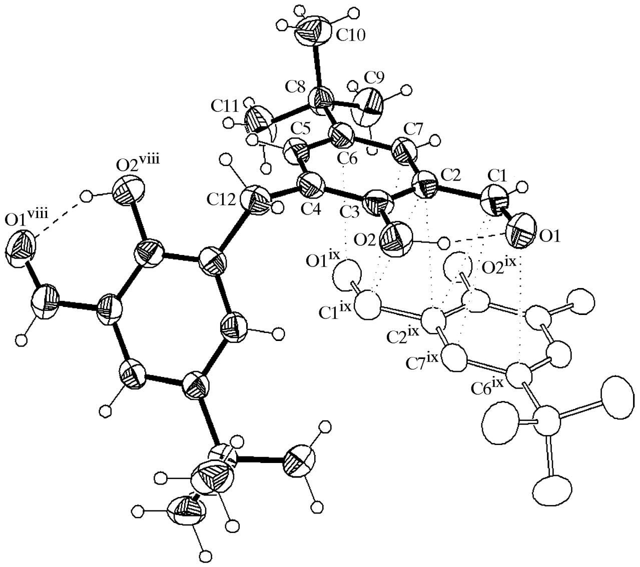

Figure 5
A view of the structure of polymorph (IV*a*); intramolecular hydrogen-bonding interactions between the phenol and aldehyde functions are shown as dashed lines. Dotted lines show interatomic distances in the range 3.42–3.47 Å in the π–π overlap region. Displacement ellipsoids are drawn at the 50% probability level. [Symmetry codes: (viii) $2 - x$, $\frac{3}{2} - y$, z; (ix) $2 - x$, $1 - y$, $-z$.]

In form (IV*a*), the molecules are packed as shown in Figs. 5 and 7. In contrast to the previous report of this structure (Masci *et al.*, 2004), we have identified π–π interactions (the most direct overlap being between the sections containing atoms O1/C1/C2/C7/C6; see Fig. 5) linking the molecules into sets of zigzag ribbons running parallel to either the *a* or the *b* axis. As can be seen in Fig. 5, π-stacked pairs of rings are parallel and related by inversion; the distance between the mean plane of the benzaldehyde ring containing atoms O1 and C7 and the centroid of the neighbouring phenyl ring at $(2 - x, 1 - y, -z)$ is 3.361 (4) Å.

In polymorph (IV*b*), the two independent molecules form *ABAB* π-stacked columns parallel to the *b* axis (Fig. 8). The relative rotation between adjacent layers prevents steric interference between successive *tert*-butyl groups (Fig. 6). The benzaldehyde rings are almost parallel [interplanar angle = 6.34 (10)°], with average interplanar separations of 3.48 and 3.32 Å between the ring containing atoms O1 and C7 and that containing O3 and C19 at $(-x, y, \frac{1}{2} - z)$ and $(-x, 1 + y, \frac{1}{2} - z)$, respectively. Again, the shortest π–π interactions are between the carbonyl groups and the phenyl rings of neighbouring molecules in the stack.

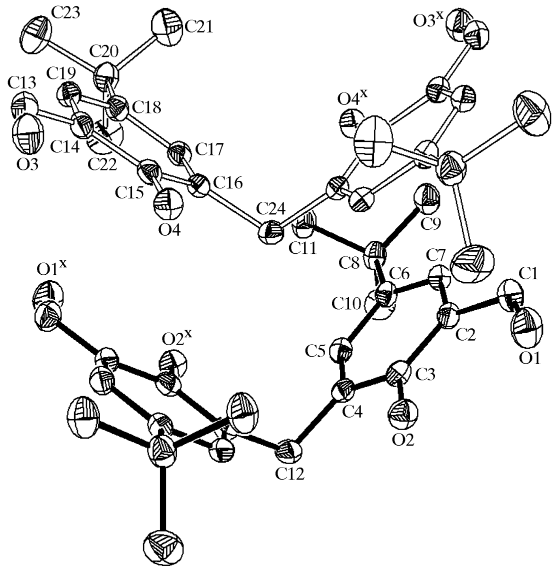

Figure 6
A view of the two independent molecules in polymorph (IV*b*). A twofold axis passes through atoms C12 and C24. Displacement ellipsoids are drawn at the 30% probability level. [Symmetry code: (x) $-x, y, \frac{1}{2} - z$.]

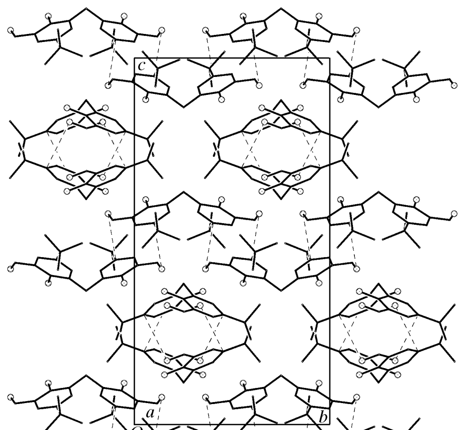

Figure 7
A unit-cell plot for polymorph (IV*a*), viewed down the *a* axis, showing the π–π-stacked ribbons running parallel to *a* and parallel to *b*. O atoms are shown as shaded circles. Dashed lines indicate the π–π overlapped sections.

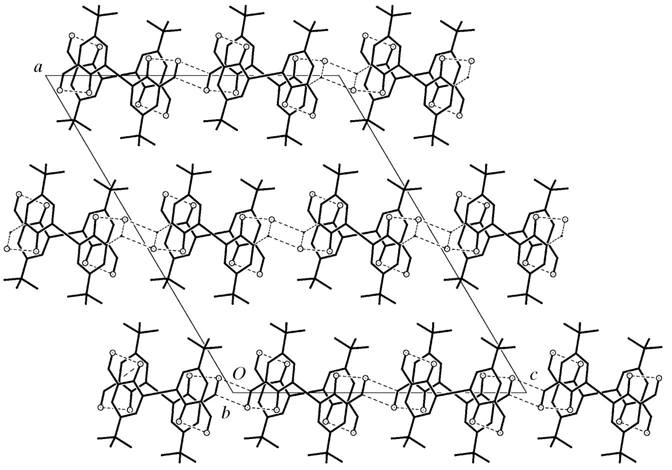

Figure 8
A unit-cell plot for polymorph (IV*b*), projected down *b*, showing π-stacked columns parallel to *b* and inter- and intramolecular hydrogen bonding (dashed lines). O atoms are shown as shaded circles.

Experimental

Compound (I) was synthesized according to the procedure of Dhawan & Gutsche (1983). For the synthesis of (II), compound (I) (10 g, 27 mmol), allyl bromide (7 g, 58 mmol), anhydrous K_2CO_3 (7.42 g) and acetone (100 ml) were placed in a 250 ml three-necked round-bottomed flask fitted with a reflux condenser and a sealed stirrer unit, and were refluxed for 20 h with stirring. The reaction mixture was then poured into water (200 ml) and the aqueous layer was extracted three times with diethyl ether. The organic layer was washed with a 2 *M* sodium hydroxide solution and dried over anhydrous K_2CO_3. The solvent was removed under vacuum, leaving a white solid, which was recrystallized from dichloromethane/*n*-hexane; the yield was 9.0 g (74%). Colourless crystals suitable for X-ray studies were obtained by slow evaporation of a solution of dichloromethane/pentane (1:5). Thin-layer chromatography (TLC) on silica gel (diethyl ether/petroleum ether 40/60, 45:55): $R_F = 0.68$. Analysis calculated for (II)·$0.5H_2O$: C 75.45, H 8.95%; found: C 75.64, H 9.06%. ^{1}H NMR ($CDCl_3$, p.p.m.): 7.24 (*d*, 2H, ArH), 7.01 (*d*, 2H, ArH), 6.07 (*m*, 2H, allyl =CH), 5.34 (*dd*, 2H, allyl =CH_2), 5.30 (*dd*, 2H, allyl =CH_2), 4.73 (*d*, 4H, CH_2OH), 4.34 (*d*, 4H, allyl CH_2), 4.70 (*s*, 4H, CH_2OH), 4.07 (*s*, 2H, $ArCH_2Ar$), 1.26 [*s*, 18H, $C(CH_3)_3$]. IR (KBr, cm^{-1}): 3272 [*s*, ν(OH)], 3081 [*w*, ν(allyl =CH_2)], 883 (*m*, 1,2,3,5 tetrasubstitution of Ar).

Compound (III) was synthesized by a method similar to that reported by Taniguchi (1984). Activated MnO_2 (50 g) was added to a solution of (II) (9 g, 20 mmol) in chloroform (200 ml). The reaction mixture was refluxed for 19–20 h, after which time MnO_2 was filtered off and the organic layer dried over anhydrous $MgSO_4$. The solvent was removed under vacuum, leaving a pale-yellow oil that crystallized under vacuum over a period of one week. The solid was then washed with cold methanol to remove the yellow impurities. Colourless crystals suitable for X-ray studies were obtained by slow evaporation of a diethyl ether solution of the product. The yield was 7.0 g (78%). TLC on silica gel (diethyl ether/petroleum ether 40/60, 30:70): R_F = 0.50. Analysis calculated for (III)·0.5H$_2$O: C 76.11, H 8.15%; found: C 76.08, H 8.15%. ^{1}H NMR (CDCl$_3$, p.p.m.): 10.4 (*s*, 2H, CHO), 7.75 (*d*, 2H, ArH), 7.30 (*d*, 2H, ArH), 6.06 (*m*, 2H, allyl =CH), 4.40 (*dd*, 2H, allyl =CH$_2$), 4.44 (*dd*, 2H, allyl =CH$_2$), 4.13 (*s*, 2H, ArCH$_2$Ar), 1.26 [*s*, 18H, C(CH$_3$)$_3$]. IR (KBr, cm^{-1}): 1660 [ν(C=O)], 3081 [*w*, ν(allyl =CH$_2$)], 885 (*m*, 1,2,3,5 tetrasubstitution of Ar).

Compound (IV) was obtained using the method described by Boss & Scheffold (1976). To a solution of (III) (7 g, 15.6 mmol) in ethanol (150 ml) were added 10% Pd on activated charcoal (1.5 g) and *p*-toluenesulfonic acid (0.7 g) in water (5 ml). The stirred suspension was refluxed for 2 d, after which time the reaction mixture was filtered hot. On cooling, the product precipitated out as a pale-yellow powder, which was filtered off (yield 1 g). An additional portion of (IV) (3 g) was obtained on concentration of the resulting filtrate. Pale-yellow crystals of (IV*a*) suitable for X-ray studies were obtained by slow evaporation from a solution of the product in diethyl ether. The yield was 4 g (70%). TLC on silica gel (diethyl ether/petroleum ether 40/60, 30:70): R_F = 0.64. Analysis calculated: C 74.97, H 7.66%; found: C 74.51, H 7.86%. ^{1}H NMR (CDCl$_3$, p.p.m.): 11.19 (*s*, 2H, Ar—OH), 9.86 (*s*, 2H, CHO), 7.64 (*d*, 2H, ArH), 7.37 (*d*, 2H, ArH), 4.03 (*s*, 2H, ArCH$_2$Ar), 1.26 [*s*, 18H, C(CH$_3$)$_3$]. IR (KBr, cm^{-1}): 1658 [ν(C=O)], 1270 [*s*, ν(ArOH)], 1216 (*s*).

Compound (II)

Crystal data

$C_{29}H_{40}O_4$
M_r = 452.61
Triclinic, $P\overline{1}$
a = 10.6025 (11) Å
b = 11.9199 (12) Å
c = 12.4180 (13) Å
α = 64.611 (2)°
β = 82.672 (2)°
γ = 66.330 (2)°
V = 1296.7 (2) Å^3

Z = 2
D_x = 1.159 Mg m^{-3}
Mo $K\alpha$ radiation
Cell parameters from 2476 reflections
θ = 2.3–27.2°
μ = 0.08 mm^{-1}
T = 150 (2) K
Block, colourless
0.29 × 0.17 × 0.12 mm

Data collection

Bruker SMART 1000 CCD area-detector diffractometer
φ and ω scans
Absorption correction: multi-scan (*SADABS*; Sheldrick, 2001)
$T_{\rm min}$ = 0.938, $T_{\rm max}$ = 1.000
9408 measured reflections

4565 independent reflections
3085 reflections with $I > 2\sigma(I)$
$R_{\rm int}$ = 0.025
$\theta_{\rm max}$ = 25.0°
$h = -12 \rightarrow 12$
$k = -14 \rightarrow 14$
$l = -14 \rightarrow 14$

Refinement

Refinement on F^2
$R[F^2 > 2\sigma(F^2)]$ = 0.057
$wR(F^2)$ = 0.173
S = 1.04
4565 reflections
310 parameters
H-atom parameters constrained

$w = 1/[\sigma^2(F_o^2) + (0.0843P)^2 + 0.7234P]$
where $P = (F_o^2 + 2F_c^2)/3$
$(\Delta/\sigma)_{\rm max} < 0.001$
$\Delta\rho_{\rm max}$ = 0.69 e Å^{-3}
$\Delta\rho_{\rm min}$ = −0.22 e Å^{-3}

Table 1
Hydrogen-bonding geometry (Å, °) for (II).

D—H···A	D—H	H···A	D···A	D—H···A
O1—H1OA···O4$^{\rm i}$	0.83	1.93	2.744 (3)	166
O1—H1OB···O4$^{\rm iv}$	0.82	1.99	2.749 (2)	155
O4—H4OA···O1$^{\rm iv}$	0.91	1.85	2.749 (2)	167
O4—H4OB···O1$^{\rm v}$	0.84	1.90	2.744 (3)	177

Symmetry codes: (i) $1 + x, y, z$; (iv) $-x, 1 - y, -z$; (v) $x - 1, y, z$.

Table 2
Hydrogen-bonding geometry (Å, °) for (III).

D—H···A	D—H	H···A	D···A	D—H···A
C5—H5···O1$^{\rm vii}$	0.95	2.46	3.406 (2)	171
C14—H14···O4$^{\rm vi}$	0.95	2.62	3.560 (2)	170

Symmetry codes: (vi) $x, \frac{1}{2} - y, \frac{1}{2} + z$; (vii) $x, \frac{1}{2} - y, -\frac{1}{2} + z$.

Compound (III)

Crystal data

$C_{29}H_{36}O_4$
M_r = 448.58
Monoclinic, $P2_1/c$
a = 16.2931 (10) Å
b = 10.1951 (6) Å
c = 16.4318 (10) Å
β = 108.367 (1)°
V = 2590.4 (3) Å^3
Z = 4

D_x = 1.150 Mg m^{-3}
Mo $K\alpha$ radiation
Cell parameters from 7890 reflections
θ = 2.4–23.3°
μ = 0.08 mm^{-1}
T = 150 (2) K
Block, colourless
0.26 × 0.16 × 0.14 mm

Data collection

Bruker SMART 1000 CCD area-detector diffractometer
ω scans
Absorption correction: multi-scan (*SADABS*; Sheldrick, 2001)
$T_{\rm min}$ = 0.900, $T_{\rm max}$ = 1.000
17 928 measured reflections
4559 independent reflections

3620 reflections with $I > 2\sigma(I)$
$R_{\rm int}$ = 0.020
$\theta_{\rm max}$ = 25.0°
$h = -19 \rightarrow 19$
$k = -12 \rightarrow 12$
$l = -19 \rightarrow 19$

Refinement

Refinement on F^2
$R[F^2 > 2\sigma(F^2)]$ = 0.043
$wR(F^2)$ = 0.123
S = 1.02
4559 reflections
317 parameters
H-atom parameters constrained

$w = 1/[\sigma^2(F_o^2) + (0.058P)^2 + 1.0861P]$
where $P = (F_o^2 + 2F_c^2)/3$
$(\Delta/\sigma)_{\rm max}$ = 0.001
$\Delta\rho_{\rm max}$ = 0.29 e Å^{-3}
$\Delta\rho_{\rm min}$ = −0.18 e Å^{-3}

Polymorph (IV*a*)

Crystal data

$C_{23}H_{28}O_4$
M_r = 368.45
Tetragonal, $I4_1/a$
a = 12.7930 (7) Å
c = 24.158 (2) Å
V = 3953.7 (4) Å^3
Z = 8
D_x = 1.238 Mg m^{-3}

Mo $K\alpha$ radiation
Cell parameters from 3205 reflections
θ = 2.8–22.8°
μ = 0.08 mm^{-1}
T = 150 (2) K
Tablet, yellow
0.28 × 0.20 × 0.05 mm

Data collection

Bruker SMART 1000 CCD area-detector diffractometer
φ and ω scans
Absorption correction: multi-scan (*SADABS*; Sheldrick, 2001)
$T_{\rm min}$ = 0.931, $T_{\rm max}$ = 1.000
19 093 measured reflections

1736 independent reflections
1203 reflections with $I > 2\sigma(I)$
$R_{\rm int}$ = 0.056
$\theta_{\rm max}$ = 25.0°
$h = -15 \rightarrow 15$
$k = -15 \rightarrow 15$
$l = -28 \rightarrow 28$

Refinement

Refinement on F^2
$R[F^2 > 2\sigma(F^2)]$ = 0.043
$wR(F^2)$ = 0.120
S = 1.04
1736 reflections
125 parameters
H-atom parameters constrained

$w = 1/[\sigma^2(F_o^2) + (0.0446P)^2 + 4.6694P]$
where $P = (F_o^2 + 2F_c^2)/3$
$(\Delta/\sigma)_{\rm max} < 0.001$
$\Delta\rho_{\rm max}$ = 0.19 e Å^{-3}
$\Delta\rho_{\rm min}$ = −0.21 e Å^{-3}

Polymorph (IV*b*)

Crystal data

$C_{23}H_{28}O_4$
$M_r = 368.45$
Monoclinic, $C2/c$
$a = 26.809$ (2) Å
$b = 8.4543$ (7) Å
$c = 21.3720$ (18) Å
$\beta = 120.618$ (1)°
$V = 4168.7$ (6) Å^3
$Z = 8$
$D_x = 1.174$ Mg m^{-3}
Mo $K\alpha$ radiation
Cell parameters from 3051 reflections
$\theta = 2.6$–25.6°
$\mu = 0.08$ mm^{-1}
$T = 153$ (2) K
Tablet, light brown
0.48 × 0.38 × 0.16 mm

Data collection

Bruker SMART 1000 CCD area-detector diffractometer
φ and ω scans
Absorption correction: multi-scan (*SADABS*; Sheldrick, 2001)
$T_{\min} = 0.919$, $T_{\max} = 1.000$
14 739 measured reflections
3668 independent reflections
2235 reflections with $I > 2\sigma(I)$
$R_{\rm int} = 0.049$
$\theta_{\max} = 25.0$°
$h = -31 \rightarrow 31$
$k = -10 \rightarrow 10$
$l = -25 \rightarrow 25$

Refinement

Refinement on F^2
$R[F^2 > 2\sigma(F^2)] = 0.047$
$wR(F^2) = 0.132$
$S = 1.01$
3668 reflections
251 parameters
H atoms treated by a mixture of independent and constrained refinement
$w = 1/[\sigma^2(F_o^2) + (0.0393P)^2 + 4.8718P]$ where $P = (F_o^2 + 2F_c^2)/3$
$(\Delta/\sigma)_{\max} < 0.001$
$\Delta\rho_{\max} = 0.20$ e Å^{-3}
$\Delta\rho_{\min} = -0.18$ e Å^{-3}

Table 3
Hydrogen-bonding geometry (Å, °) for (IV*a*).

D—H···A	D—H	H···A	D···A	D—H···A
O2—H2···O1	0.92 (2)	1.80 (2)	2.645 (2)	151 (2)

Table 4
Hydrogen-bonding geometry (Å, °) for (IV*b*).

D—H···A	D—H	H···A	D···A	D—H···A
O2—H2···O1	0.94 (2)	1.81 (2)	2.625 (3)	144 (2)
O4—H4···O3	0.88 (2)	1.85 (2)	2.631 (2)	147 (2)
C13—H13···O3$^{\rm ii}$	0.95	2.57	3.454 (3)	156

Symmetry code: (ii) $-x, 2-y, 1-z$.

Except as described below, H atoms bonded to C atoms were placed at calculated positions and refined using a riding model. The constrained C—H distances were 0.95, 0.98, 0.99 and 0.99 Å for aryl, methyl, methylene and ethylene H atoms, respectively. The $U_{\rm iso}$(H) values were set at $1.2U_{\rm eq}$(C) for methylene and aryl H atoms, and at $1.5U_{\rm eq}$(C) for *tert*-butyl H atoms. For (II), the disordered H atoms bonded to atoms O1 and O4 were located from difference maps and were not further refined; their $U_{\rm iso}$(H) values were fixed at 0.04 Å^2. The $U_{\rm iso}$(H) values of the *tert*-butyl H atoms were fixed at 0.05 Å^2, and those of the H atoms on atoms C27 and C24 at 0.04 Å^2. For (IV*a*), H atoms bonded to O atoms were placed at calculated positions, with a constrained O—H distance of 0.84 Å and with $U_{\rm iso}$(H) set at $1.5U_{\rm eq}$ of the carrier O atom. In (IV*b*), the $U_{\rm iso}$ values for the *tert*-butyl H atoms were fixed at 0.05 Å^2, while the phenol H atoms were located from difference maps and their positions refined, with $U_{\rm iso}$(H) values fixed at 0.05 Å^2.

For all determinations, data collection: *SMART* (Bruker, 1998); cell refinement: *SMART*; data reduction: *SAINT* (Bruker, 1998); program(s) used to solve structure: *SHELXTL* (Sheldrick, 2001); program(s) used to refine structure: *SHELXTL*; molecular graphics: *SHELXTL*; software used to prepare material for publication: *SHELXTL*.

The authors thank Professor M. A. McKervey and Dr H. Q. N. Gunaratne, CSS Limited, for helpful discussions.

Supplementary data for this paper are available from the IUCr electronic archives (Reference: BM1580). Services for accessing these data are described at the back of the journal.

References

Barreira Fontecha, J., Goetz, S. & McKee, V. (2002). *Angew. Chem. Int. Ed.* **41**, 4554–4556.
Boss, R. & Scheffold, R. (1976). *Angew. Chem.* **88**, 578–579.
Bruker (1998). *SMART* and *SAINT*. Bruker AXS Inc., Madison, Wisconsin, USA.
Dhawan, B. & Gutsche, C. D. (1983). *J. Org. Chem.* **48**, 1536–1539.
Masci, B., Levi Mortera, S., Seralessandri, L. & Thuery, P. (2004) *Acta Cryst.* C**60**, o107–o109.
Sheldrick, G. M. (2001). *SHELXTL* (Version 6.12) and *SADABS* (Version 6.12). Bruker AXS Inc., Madison, Wisconsin, USA.
Taniguchi, S. (1984). *Bull. Chem. Soc. Jpn*, **57**, 2683–2684.